applied sciences

MDPI

Article

A Novel Reference Governor for Disturbance Observer-Based Load Pressure Control in a Dual-Actuator-Driven Electrohydraulic Actuator

Guisheng Zhao [1], Shaonan Chen [1,*], Yixiang Liu [2] and Kai Guo [3]

[1] China Nuclear Power Technology Research Institute, Shenzhen 518031, China
[2] Department of Control Science and Engineering, Shandong University, Jinan 250061, China
[3] The Key Laboratory of High Efficiency and Clean Mechanical Manufacture of Ministry of Education, Department of Mechanical Engineering, Shandong University, Jinan 250061, China
* Correspondence: chenshaonan@cgnpc.com.cn

Abstract: In real-world applications, hydraulic pressure control performance is influenced by model uncertainties, the control bandwidths of valves and pumps, and deviations from the linear working region. To overcome the aforementioned obstacles, a novel reference governor for disturbance observer (DOB)-based load pressure control is proposed in this paper for a dual-actuator-driven electrohydraulic cylinder. First, a control-oriented model for load pressure control was developed. On the basis of this, a nonlinear DOB-based feedback controller, as well as a mid-range control architecture for the variable displacement pump and proportional valve, was fabricated so that the performance degradation caused by the pump's slow responses and imprecise system parameters is suppressed. Specifically, this controller is augmented by a novel smooth reference governor, which modifies the load pressure command in the pressure transition periods to guarantee that the actuator's constraints are not violated. Another merit of the novel reference governor is that it ensures a smooth trajectory transition, and therefore, unmodeled high-frequency plant dynamics will not be invoked. Case studies were carried out to verify the effectiveness of the proposed control approach. The study results show that the approach can significantly enhance the hydraulic system's pressure tracking performance.

Keywords: reference governor; electrohydraulic system; parameter uncertainty; disturbance

Citation: Zhao, G.; Chen, S.; Liu, Y.; Guo, K. A Novel Reference Governor for Disturbance Observer-Based Load Pressure Control in a Dual-Actuator-Driven Electrohydraulic Actuator. *Appl. Sci.* **2022**, *12*, 8367. https://doi.org/10.3390/app12168367

Academic Editor: Subhas Mukhopadhyay

Received: 17 July 2022
Accepted: 16 August 2022
Published: 21 August 2022

1. Introduction

Electrohydraulic systems are currently utilized extensively in a variety of industrial and transport applications [1–6], e.g., construction machines [7], robot manipulators [8], load simulators [9], and steering systems [10]. Hydraulic pressure control performance is critical in particular situations, e.g., tunneling boring machine thrust force control and hydraulic press forming force control. In general, two kinds of hydraulic system configurations are used for these applications. One feasible method is to regulate the supply flow to the cylinder chamber by using an electrohydraulic servo/proportional valve [1,11–15], which enables satisfactory dynamic behavior. Another approach is to regulate flow using a variable flow pump; this solution offers better energy efficiency [16], but the system bandwidth is restricted by the response speed of the pump, in which the moving parts' inertia is much larger than that of the servo/proportional valve.

A solution was proposed by combining an electrohydraulic servo valve with a variable displacement pump [17]. In this configuration, the pump drives the cylinder together with the valve. To obtain better dynamic performance for electrohydraulic cylinder control, various control methods have been used [18–20]. A strategy featuring double closed-loop compound robust control was proposed to deal with the underperformance of double pump–double valve-controlled motors due to external interference, such as poor stability

of output speed, low controllability, and difficulties in managing synchronous output [21]. A sliding-mode controller of a single-channel motor was designed for the inner loop, while double-channel cross-coupled closed-loop control was applied to the outer loop. A novel pump–valve compound drive system was designed in [22], and a force control method combining tracking error compensation and load compensation control was designed. In [23], a time-sharing controller was proposed for motor pump–valve control systems. During the high-flow period, the cylinder is controlled by adjusting the speed of the control motor, while during the low-flow period, the cylinder is controlled by the form of the valve-controlled cylinder. Valve–pump parallel variable mode control for hydraulic speed regulation systems, which established a flexible control mechanism using pump control and valve control, was proposed in [24]. In [25], valve–pump parallel variable structure control was proposed for a variable speed hydraulic system. Leaking parallel valve control was applied to improve low-speed performance at the start and stop stages by increasing damping ratios and compensating for the reduction in damping ratios due to the negative friction slope. In these studies, linear control strategies were employed, but the control performance was often unsatisfying if the working conditions varied dramatically [26]. To increase tracking performance, sliding mode control was used for electrohydraulic cylinder pressure control [27–29], but chattering phenomena may excite unwanted frequency modes and degrade the tracking performance. Wang [11] showed that by accounting for the nonlinear behavior and parameter uncertainties of the plant, a high tracking performance could be achieved, and this control strategy was also verified in [30,31]. In general, many control strategies for a dual-actuator-driven electrohydraulic actuator mainly focus on parameter uncertainties and disturbances in the system, but the actuator constraints, e.g., the stroke and velocity limit of the control valve and variable displacement pump, are not considered. If these constraints are violated, the closed-loop system control performance will significantly degrade.

Figure 1 depicts the electrohydraulic system considered in this paper. It consists of a proportional valve and variable displacement pump. During pressure transition, the cylinder load flow can be tuned quickly with the help of the proportional valve, while in the steady state, the valve spool can be shifted to the midpoint, and the variable displacement pump can maintain the cylinder pressure. This hydraulic configuration can help to improve system transient behavior while preserving the benefits of the pump control system.

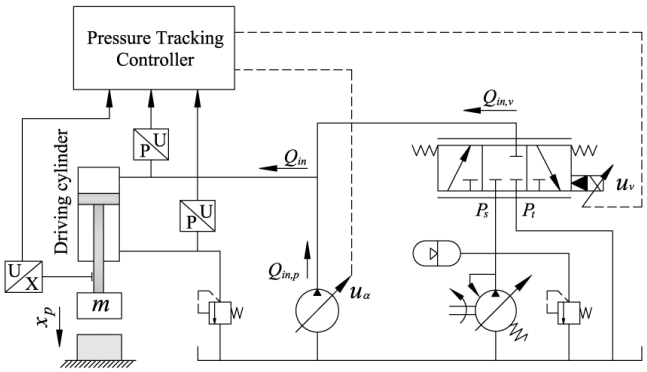

Figure 1. Schematic diagram of the hydraulic system.

To deal with the aforementioned problems, a novel reference governor for disturbance observer-based load pressure control in a dual-actuator-driven electrohydraulic actuator is proposed. First, the reference governor is used to synthesize an adaptive controller by explicitly taking into account the actuator constraints without the need for the careful selection of feedback gains or gain scheduling techniques. In addition, disturbance observers or adaptive controllers proposed in [27,32] can be used. The proposed approach can be extended to consider additional constraints, e.g., the proportional valve performance limit. The main contributions of this article are two-fold, as follows:

(1) The proposed load pressure tracking controller can estimate the plant's lumped disturbance caused by uncertain parameters to improve the robustness of the closed-loop system. In addition, a mid-range controller that dynamically allocates the command to the pump and proportional valve is used, which can make the best of the higher bandwidth of the proportional valve and keep the valve position close to the midpoint of its range.

(2) A novel reference governor is augmented to ensure that the rate and magnitude constraints of the pump and the valve are not violated. If constraint violation is foreseen, the pressure reference trajectory will be reduced. The proposed method can generate smoother pressure trajectories than nominal reference governors, and therefore, it will not excite high-frequency modes, which helps to improve the model accuracy used in the prediction.

The remaining sections are organized as follows. In Section 2, the mathematical model is presented. Section 3 describes the nonlinear controller, including the mid-range controller and the innovative smooth reference governor. In Section 4, a case study demonstrating the effectiveness of the proposed controller is presented. Finally, conclusions are drawn in Section 5.

2. Mathematical Modeling

The analyzed system is depicted in Figure 1. The dynamics of the piston of the cylinder can be described by:

$$m\ddot{x}_p = P_1 A_1 - P_2 A_2 - F_l \tag{1}$$

where m is the mass of the load, x_p is the displacement of the cylinder, P_1 and P_2 are the pressures in the forward and return chambers of the cylinder, A_1 is the piston area in the non-rod chamber, A_2 is the piston area in the rod chamber, and the overall load force is denoted by F_l.

The dynamics of the cylinder's pressure can be expressed as [33]:

$$\frac{V_{01} + A_1 x_p}{\beta_e}\dot{P}_1 = Q_{in} - A_1\dot{x}_p - C_t(P_1 - P_2) \tag{2}$$

where V_{01} and V_{02} are the total control volumes of the cylinder and the hoses connecting the cylinder to the valve, respectively, β_e is the bulk modulus of oil, C_t is the internal leakage coefficient, and the flow rate Q_{in} is given in [34] as the following equation:

$$Q_{in} = Q_{in,p} + Q_{in,v} = k_p\alpha + k_q x_v[s_g(x_v)\sqrt{P_s - P_1} + s_g(-x_v)\sqrt{P_1 - P_t}] \tag{3}$$

where $Q_{in,p}$ is the flow rate of the pump, and $Q_{in,v}$ is the flow rate of the valve.

We define the function

$$s_g(x) = \begin{cases} 1, \text{ if } x \geq 0 \\ 0, \text{ if } x < 0 \end{cases} \tag{4}$$

where the pump flow gain k_p is a constant when the pump rotation speed is fixed, α is the swashplate angle, k_q is the flow gain of the servo valve, x_v is the valve spool displacement, P_s is the discharge pressure of the pump, and P_t is the tank pressure.

In this paper, the swashplate angle dynamics is modeled using second-order dynamic systems, and the pump swashplate angle's magnitude and rate limitations are considered. The angle dynamics is given as

$$\ddot{\alpha} = 2\xi_\alpha\omega_\alpha\left[S_R\left(\frac{\omega_\alpha^2}{2\xi_\alpha\omega_\alpha}(S_M(u_\alpha) - \alpha)\right) - \dot{\alpha}\right] \tag{5}$$

where u_α is the swashplate angle, ω_α and ξ_α represent the natural frequency and damping ratio of the system, and $S_M(\cdot)$ and $S_R(\cdot)$ are constraints on the magnitude and the rate. They are defined by:

$$S_M(x) = \begin{cases} M & \text{if } x \geq M \\ x & \text{if } |x| < M \\ -M & \text{if } x \leq -M \end{cases} \tag{6}$$

The transfer function, defined as the relationship between the input u_α and the swashplate angle α, is expressed as

$$\frac{\alpha(s)}{u_\alpha(s)} = \frac{\omega_\alpha^2}{s^2 + 2\xi_\alpha \omega_\alpha s + \omega_\alpha^2} \tag{7}$$

The proportional valve dynamics can be modeled as:

$$\ddot{x}_v = 2\xi_v \omega_v \left[S_R\left(\frac{\omega_v^2}{2\xi_v \omega_v} (S_M(k_x u_v) - x_v) \right) - x_v \right] \tag{8}$$

where u_v is the input command, and ω_v and ξ_v represent the natural frequency and damping ratio of the valve.

We define $\mathbf{x} = [x_1, x_2, x_3, x_4, x_5, x_6, x_7]^T = [x_p, \dot{x}_p, P_1, \alpha, \dot{\alpha}, x_v, \dot{x}_v]^T$. The system is expressed as

$$\begin{aligned} \dot{x}_1 &= x_2 \\ \dot{x}_2 &= \tfrac{1}{m}[A_1 x_3 - A_2 P_2 - F_l] \\ \dot{x}_3 &= h(x_1)[-A_1 x_2 - C_t(x_3 - P_2) + Q_{in}(x_3, x_4, x_6)] \\ \dot{x}_4 &= x_5 \\ \dot{x}_5 &= 2\xi_\alpha \omega_\alpha \left[S_R\left(\tfrac{\omega_\alpha^2}{2\xi_\alpha \omega_\alpha} (S_M(u_\alpha) - x_4) \right) - x_5 \right] \\ \dot{x}_6 &= x_7 \\ \dot{x}_7 &= 2\xi_v \omega_v \left[S_R\left(\tfrac{\omega_v^2}{2\xi_v \omega_v} (S_M(u_v) - x_6) \right) - x_7 \right] \end{aligned} \tag{9}$$

with

$$\begin{aligned} h(x_1) &= \tfrac{\beta_e}{A_1 x_1 + V_{01}} \\ Q_{in}(x_3, x_4, x_6) &= k_p x_4 + k_q x_6 g(x_3, x_6) \\ g(x_3, x_6) &= s_g(x_6)\sqrt{P_s - x_3} + s_g(-x_6)\sqrt{x_3 - P_t} \end{aligned} \tag{10}$$

The nonlinear model shown (9) is a high-order, i.e., seventh-order, model, which makes it hard to use this form to synthesize a model-based control strategy. In order to make the controller design much more intuitive, model in (9) should be simplified as follows [26]:

$$\begin{aligned} \dot{x} &= h(x_p)\left[-A_1 \dot{x}_p - d + Q_{in}(x, x_v, \alpha)\right] \\ h(x_p) &= \tfrac{\beta_e}{A_1 x_p + V_{01}} \\ Q_{in}(x, x_v, \alpha) &= Q_{in,p} + Q_{in,v} \\ &= k_p \alpha + k_q x_v g(x, x_v) \end{aligned} \tag{11}$$

A mid-range controller was designed to allocate Q_{in} between $Q_{in,p}$ and $Q_{in,v}$, making use of the proportional valve's higher bandwidth while retaining the proportional valve's location near the middle of its operating range so as not to violate its limit. For the considered system, many parameters are unknown or uncertain, and some are even continuously changing: e.g., the internal leakage coefficient varies with the oil temperature and cylinder rod position, and the bulk modulus of oil is based on oil pressure and air entrainment. Furthermore, accurate parameter estimation is very difficult; therefore, the parameter uncertainties and external disturbances are lumped into the term d.

3. Controller Design

3.1. Disturbance Observer

The proposed disturbance observer is used to estimate the disturbance d, which is given by:

$$\begin{aligned} \dot{\hat{x}} &= h(x_p)\left(-A_1\dot{x}_p + Q_{in,d} + \hat{d}\right) + k_1\widetilde{x}_o \\ \dot{\hat{d}} &= k_2\widetilde{x}_o \end{aligned} \tag{12}$$

where $\hat{x}$ and $\hat{d}$ are the estimates of x and d, respectively, $\widetilde{x}_o$ is the estimation error, $Q_{in,d}$ is the virtual control flow of the system, and k_1 and k_2 are control gains, respectively. The dynamics of $\widetilde{x}_o$ can be given by:

$$\dot{\widetilde{x}}_o = -k_1\widetilde{x}_o + h(x_p)\left(\widetilde{d} + \widetilde{Q}_{in}\right) \tag{13}$$

where $\widetilde{Q}_{in}$ is the control flow error, i.e., $\widetilde{Q}_{in} = Q_{in} - Q_{in,d}$.

Theorem 1. *According to the disturbance observer (12), if d is bounded, the disturbance estimation error $\widetilde{d}$is bounded and will converge exponentially to a sphere centered at the origin.*

Proof. By combining (12) and (13), one obtains

$$\begin{bmatrix} \dot{\widetilde{x}}_o \\ \dot{\widetilde{d}} \end{bmatrix} = \begin{bmatrix} -k_1 & h(x_p) \\ -k_2 & 0 \end{bmatrix} \begin{bmatrix} \widetilde{x}_o \\ \widetilde{d} \end{bmatrix} + \begin{bmatrix} h(x_p)\widetilde{Q}_{in} \\ \dot{d} \end{bmatrix} \tag{14}$$

If $k_1 > 0$ and $k_2 > 0$, then the disturbance observer is stable. Furthermore, if the actuator constraints are respected, then $\widetilde{Q}_{in}$ is bounded; therefore, the disturbance estimation error $\widetilde{d}$ is bounded. □

3.2. Pressure Tracking Strategy

The nonlinear controller includes a disturbance observer-based pressure tracking controller to design the virtual control flow to the system.

The dynamics of the tracking error $\widetilde{x}_c$ is given by:

$$\dot{\widetilde{x}}_c = h(x_p)\left[-A_1\dot{x}_p - d + Q_{in}(x_1, x_v, \alpha)\right] - \dot{x}_d \tag{15}$$

A virtual controller $Q_{in,d}$ for $\widetilde{x}_c$ is designed as:

$$Q_{in,d} = A_1\dot{x}_p - \hat{d} - \frac{c_1}{a}\widetilde{x}_c + \frac{1}{a}\dot{x}_d \tag{16}$$

where c_1 is the control gain.

As mentioned earlier, the proportional valve responds more quickly than the pump, but its stroke is limited. This paper introduces a mid-range controller for allocating the flow command between the valve and pump, utilizing the valve's wider bandwidth while maintaining the spool position close to the middle of its functional range. Based on the respective frequency characteristics of the valve and pump, two filters, a high-pass filter H_v for the valve and a low-pass filter H_p for the pump, are introduced:

$$\begin{aligned} H_p(s) &= \frac{Q_{p,d}}{Q_{in,d}} = \frac{2\zeta_{da}T_{da}s+1}{T_{da}^2s^2+2\zeta_{da}T_{da}s+1} \\ H_v(s) &= \frac{Q_{v,d}}{Q_{in,d}} = \frac{T_{da}^2s^2}{T_{da}^2s^2+2\zeta_{da}T_{da}s+1} \end{aligned} \tag{17}$$

Therefore, we can obtain:

$$\alpha(s) = H_p(s)\alpha_p(s) + H_v(s)\alpha_v(s) \tag{18}$$

where $\alpha(s)$, $\alpha_p(s)$ and $\alpha_v(s)$ are the transfer functions between the actual supply flow of the cylinder chamber and the virtual command flow, the real pump flow and the desired pump flow, and the actual valve flow and the ideal valve flow, respectively.

When in the low-frequency range, the pump and valve supply flow can easily track the desired flow, i.e., $\alpha_p(s) \approx 1$, $\alpha_v(s) \approx 1$, and we can obtain

$$\alpha(s) \approx H_p(s) \cdot 1 + H_v(s) \cdot 1 \approx H_p + H_v = 1 \tag{19}$$

Similarly, when in the high-frequency range, we can obtain

$$\alpha(s) \approx H_p(s) \cdot 0 + H_v(s) \cdot 1 \approx H_v(s) \approx 1 \tag{20}$$

Therefore, $\alpha(s)$ is approximately constant.

The variable displacement angle command is given as follows:

$$\alpha_d = \frac{Q_{p,d}}{k_p} \tag{21}$$

From (10), the valve control voltage is given by

$$u_v = \begin{cases} \frac{Q_{v,d}}{k_q k_x \sqrt{P_s - x}}, & \text{if } Q_{v,d} \geq 0 \\ \frac{Q_{v,d}}{k_q k_x \sqrt{x - P_t}}, & \text{if } Q_{v,d} < 0 \end{cases} \tag{22}$$

3.3. Nominal Reference Governor

As explained in Section 2, the valve displacement and pump angle are subject to magnitude and rate saturations. Once the system leaves its linear region, the boundedness of $\widetilde{d}$ will not be guaranteed, and the disturbance estimation $\hat{d}$ will be corrupted due to actuator saturation. This problem can be alleviated by reducing the closed-loop system performance, i.e., by applying a filter to the pressure command. However, it cannot guarantee that the actuator saturation is eliminated. Another approach is to use model predictive control (MPC), which is able to exploit the entire actuator's potential while respecting the actuator constraints, but the computational cost is high, especially for the nonlinear high-order system considered here.

In this paper, a reference governor is investigated to ensure that actuator limitations are not violated by the system. If a violation of constraints is anticipated, the trajectory will be modified until all constraints are satisfied. The receding horizon principle and the bisectional search algorithm are used here to check for constraint violations, as shown in Figure 2. The command x_d is subjected to a bisectional search until the optimal modification is determined. This is implemented through the optimization of parameter α_k:

$$x_d^{rev}(k) = x_d^{rev}(k-1) + \alpha_k[x_d(k) - x_d^{rev}(k-1)] \tag{23}$$

where x_d is the target trajectory, and x_d^{rev} is the modified trajectory. When $\alpha_k = 1$, the filter does not affect the input, and conversely, when $\alpha_k = 0$, then $x_d^{rev} = x_d^{rev}(k-1)$ can be obtained. The optimal value of parameter α_k is obtained during each time interval kT_s by maintaining $x_d^{rev}(\tau) = x_d^{rev}(k)$ for $kT_s \leq \tau \leq kT_s + T_p$, where T_p is the prediction time horizon.

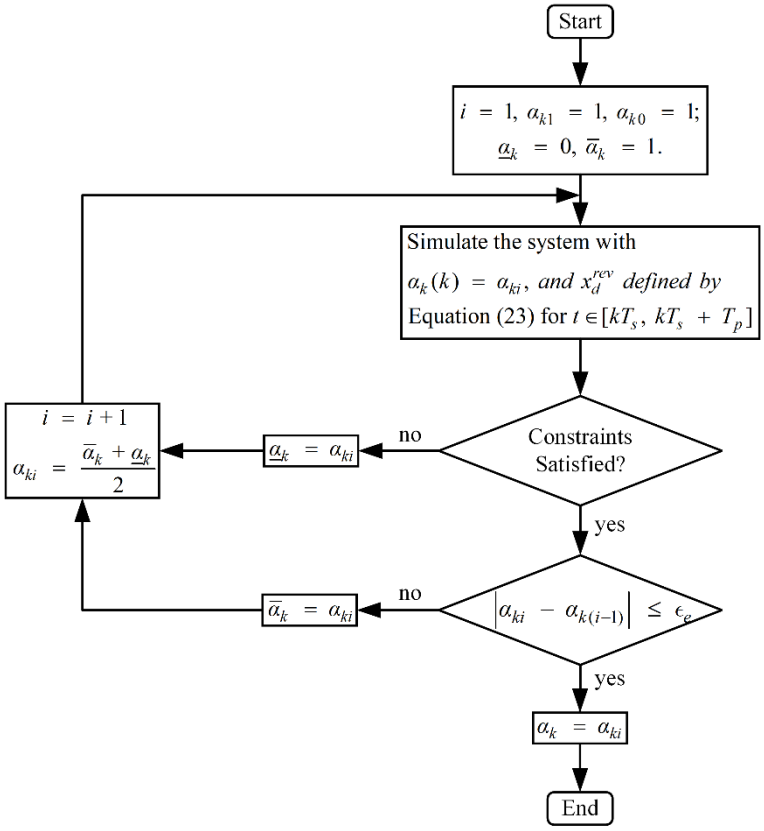

Figure 2. Bisectional search algorithm to optimize α_k.

To determine α_k at each time instant, the system in (11) including the controller dynamics in (16), (18), (21) and (22) are predicted over the interval $[kT_s, kT_s + T_p]$. α_k is decreased if constraint violations are anticipated and raised if all constraints are met. The optimal value of $\alpha_k \in [0, 1]$ is subsequently determined. The constraints considered in this paper are as follows:

$$\begin{aligned} u_v^{min} \leq u_v \leq u_v^{max} \\ u_\alpha^{\max} \leq u_\alpha \leq u_\alpha^{max} \\ \Delta u_v^{min} \leq \Delta u_v \leq \Delta u_v^{max} \\ \Delta u_\alpha^{min} \leq \Delta u_\alpha \leq \Delta u_\alpha^{max} \end{aligned} \tag{24}$$

where

$$\begin{aligned} \Delta u_v(k) = u_v(k) - u_v(k-1) \\ \Delta u_\alpha(k) = u_\alpha(k) - u_\alpha(k-1) \end{aligned} \tag{25}$$

3.4. Novel Smooth Reference Governor

Despite the advantages of the nominal reference governor, the revised trajectory is discontinuous or even jitters if the trajectory x_d changes rapidly [35]; therefore, when the discontinuous revised trajectory is applied to the closed-loop system, unmodeled high-frequency plant dynamics will be invoked, and the plant model used in the reference governor will not be accurate, which will decrease the plant behavior prediction accuracy. In this paper, a novel smooth reference governor is proposed to handle this problem, which can smooth the fast-changing trajectory by introducing a feedback mechanism based on the nominal reference governor; i.e., the nominal reference governor is augmented with a dynamic rate limiter, the threshold of which is closely related to α_k. The feedback mechanism of the dynamic rate limiter is shown in Figure 3 and is given as:

$$\dot{x}_{df} = S_{Mf}\left[K_f\left(x_d - x_{df}\right)\right] \tag{26}$$

where x_{df} is the pressure trajectory used as the reference governor input, K_f is the feedback gain and $S_{Mf}(\cdot)$ is the saturation function given by:

$$S_{Mf}(x) = \begin{cases} \alpha_k M_f & \text{if } x \geq \alpha_k M_f \\ x & \text{if } |x| < \alpha_k M_f \\ -\alpha_k M_f & \text{if} x \leq -\alpha_k M_f \end{cases} \quad (27)$$

where M_f is a constant.

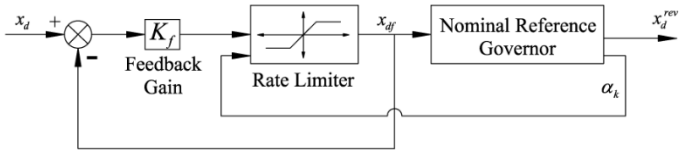

Figure 3. The schematic diagram of the smooth reference governor.

The revised trajectory from the dynamic rate limiter x_{df} is then fed to the reference governor (23). If the actuator constraints are violated, then α_k is decreased; as a result, the dynamic threshold of $S_{Mf}(\cdot)$ is then decreased, and therefore, the change rate of x_{df} is slowed down, making x_{df} smoother than that of the nominal reference governor. The smooth trajectory helps prevent the unmodeled high-frequency dynamics from happening, which improves the plant model credibility in the model prediction. Therefore, the actuator constraint violation prediction accuracy is improved.

The block diagram of the proposed control structure is shown in Figure 4. As shown, the proposed smooth reference governor transforms the pressure x_d to a revised reference signal x_d^{rev}. The nonlinear feedback controller treats x_d^{rev} as the command, and then a virtual flow command $Q_{in,d}$ is generated. Finally, $Q_{in,d}$ is divided into α_d and u_v by the mid-range controller, which drive the pump and valve, respectively.

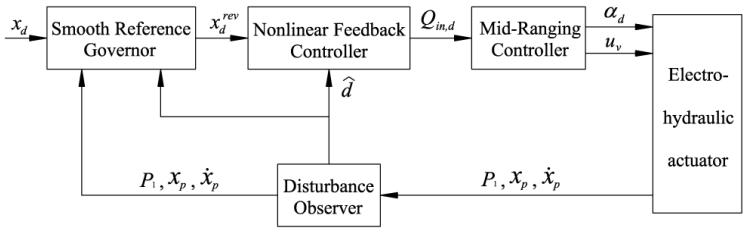

Figure 4. Block diagram of the controller structure.

4. Case Studies

In the case studies described in this section, the presented controller was applied to the electrohydraulic system of a hydraulic press, the maximum load of which is 700 kN. The dynamics of the system are defined by (9), and the system parameters of the hydraulic press are given in Table 1.

To show the efficiency of the suggested method, two case studies were carried out in a simulation, and the following three controllers were compared in the two cases:

(1) The proposed smooth reference governor-based controller (SRG);
(2) The nominal reference governor-based controller (RG);
(3) A third controller conducting pressure tracking without a reference governor. The impact of the reference governor was simulated by a first-order low-pass filter (LPF) with a 0.17 s time constant.

The selection of the control parameters of the proposed controller is based on the following rules: (1) control gains k_1, k_2 and c_1 are chosen based on the saturation limits and bandwidth of the actuator; (2) filter parameters T_{da} and ξ_{da} depend on the saturation value of the valve displacement; and (3) decreasing the sampling time T_s and increasing

the prediction time T_p can improve control performance, but more computing resources are required. According to the above rules and through trial and error, the control parameters of the proposed SRG controller were chosen for the simulation, as shown in Table 2.

Table 1. Parameters of the electrohydraulic system.

Parameter	Description	Value
m	Load mass	1200 kg
A_1	Driving cylinder piston side chamber area	3.8×10^{-2} m^2
P_s	Pump supply pressure	2.0×10^7 Pa
C_t	Driving cylinder leakage coefficient	0 m^3/(s·Pa)
β_e	Oil bulk modulus	1×10^9 Pa
$k_q \cdot k_x$	Servo valve flow gain coefficient	1.782×10^{-8} m$^3/\left(\text{s}\cdot\text{V}\cdot\sqrt{\text{Pa}}\right)$
k_p	Pump flow coefficient	6.56×10^{-3} m^3/(s·rad)
ω_α	Pump dynamics natural frequency	25 rad/s
ξ_α	Pump dynamics damping ratio	1
ω_v	Valve dynamics natural frequency	200 rad/s
ξ_v	Valve dynamics damping ratio	1

Table 2. Parameters of the controller.

Parameter	Value	Parameter	Value
k_1	200	k_2	5.43×10^{-8}
c_1	10	T_{da}	0.15
ξ_{da}	1	T_s	0.001
T_p	0.3		

Case 1: Mild Pressure Trajectory Test.

The three controllers were first tested with the trajectory shown in Figure 5. The constraints for the pump and valve were satisfied for all three controllers, and these three controllers showed almost the same performance, which can be seen in Figure 6. This is due to the relatively mild pressure trajectory, which can be tracked without aggressive actuator control. It also shows that the proposed smooth reference governor does not slow down the tracking results when the actuator constraints are not violated.

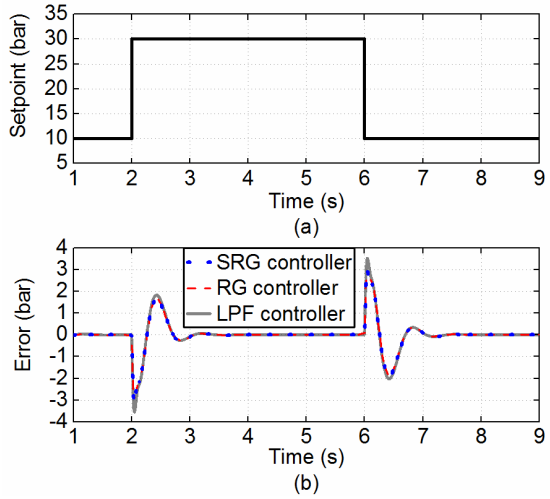

Figure 5. Tracking performance for a step trajectory from 10 bar to 30 bar. (**a**) The pressure trajectory. (**b**) The tracking error of the three controllers.

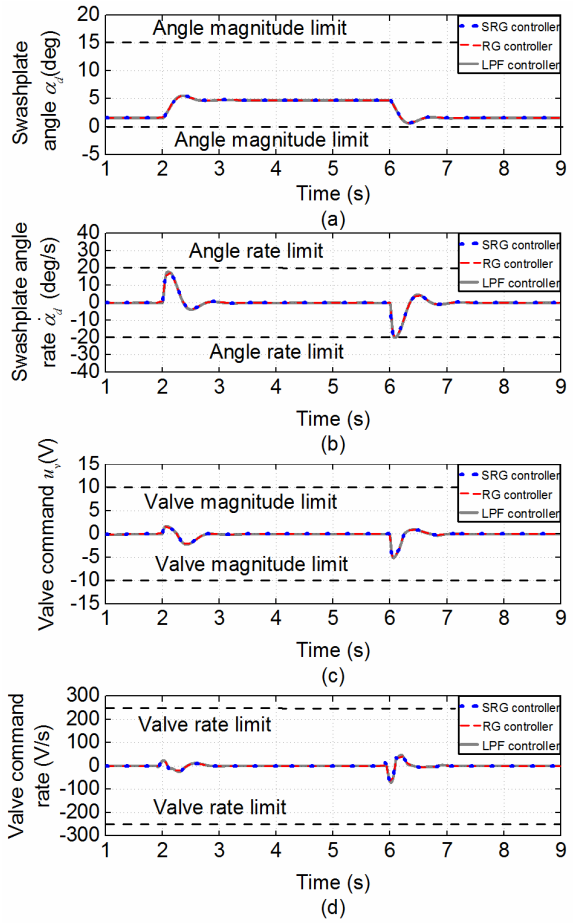

Figure 6. Actuator control inputs of the three controllers for a step trajectory from 10 bar to 30 bar. (**a**) The swashplate angle. (**b**) The swashplate angle rate. (**c**) The valve command. (**d**) The valve command rate.

Case 2: Violent Pressure Trajectory Test

Figure 7 shows the performance when a step trajectory from 10 bar to 70 bar is used. The variable displacement pump's angle rate constraint is strongly violated, leading to oscillating tracking performance if no load governor is used. Compared with the smooth reference governor, the nominal reference governor applies the pressure trajectory too aggressively, which leads to intermediate steps when α_k cannot be optimized. This results in the jittering trajectory shown in Figure 8. In addition, the constraints are slightly violated compared with the novel reference governor, as shown in Figure 9. The smooth reference governor avoids intermediate infeasible steps, and the updated trajectory is smooth and satisfies all constraints. This is due to the novel feedback mechanism inherent in the smooth reference governor, which dynamically slows down the trajectory according to α_k; this helps to avoid exciting the unexpected high-frequency dynamics of the system and helps to improve the model prediction accuracy.

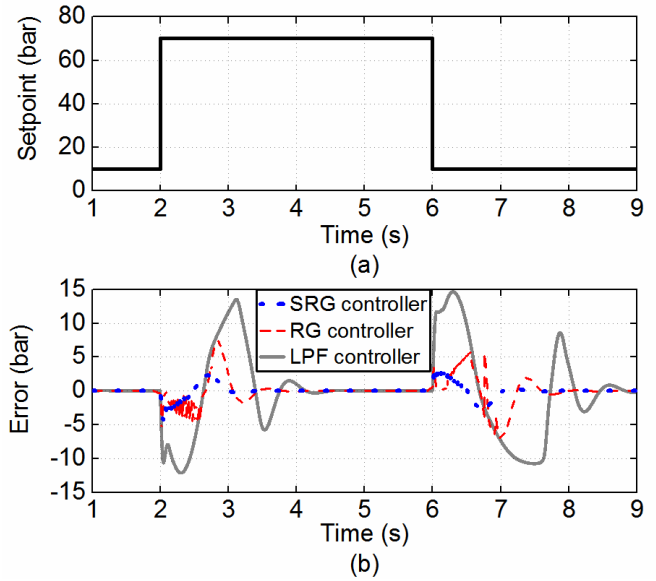

Figure 7. Tracking performance for a step trajectory from 10 bar to 70 bar. (**a**) The pressure trajectory. (**b**) The tracking error of the three controllers.

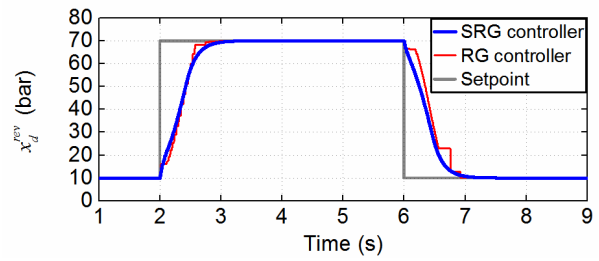

Figure 8. Trajectory used for the nonlinear DOB controller of the three controllers.

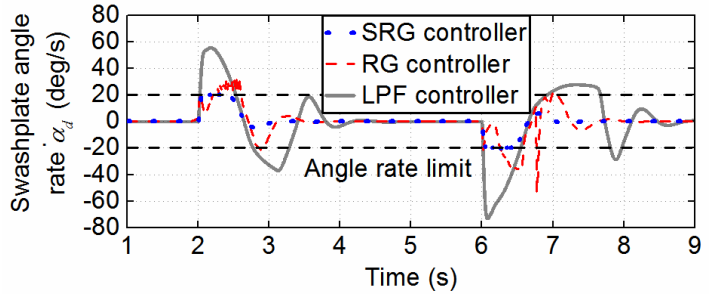

Figure 9. Actuator control inputs of the three controllers for a step trajectory from 10 bar to 70 bar.

5. Conclusions

In this paper, a DOB-based load pressure control strategy with a novel smooth reference governor is proposed for dual-actuator-driven electrohydraulic cylinders. The DOB-based feedback controller and mid-range control architecture can suppress the performance degradation caused by the pump's slow responses and imprecise system parameters. In addition, the novel smooth reference governor ensures a smooth trajectory and will not excite the unwanted high-frequency dynamics of the plant. The results of case studies show that the novel feedback mechanism of the smooth reference governor can dynamically slow down the trajectory and avoid exciting the unexpected high-frequency dynamics of the system, which helps to improve model prediction accuracy. The benefits of the novel smooth reference generator are verified by the superior tracking performance of the hydraulic system.

Author Contributions: Conceptualization, G.Z., S.C., Y.L. and K.G.; data curation, G.Z.; formal analysis, G.Z., S.C., Y.L. and K.G.; funding acquisition, Y.L. and K.G.; investigation, G.Z., S.C., Y.L. and K.G.; methodology, G.Z., S.C., Y.L. and K.G.; project administration, Y.L.; resources, Y.L.; software, Y.L.; supervision, K.G.; validation, S.C.; visualization, G.Z.; writing—original draft, G.Z., S.C., Y.L. and K.G.; writing—review and editing, G.Z., S.C., Y.L. and K.G. All authors have read and agreed to the published version of the manuscript.

Funding: This research was funded by the Key R&D Program of Shandong Province under Grant 2019GGX104008 and Grant 2019JZZY020318.

Institutional Review Board Statement: Not applicable.

Informed Consent Statement: Not applicable.

Data Availability Statement: Not applicable.

Conflicts of Interest: The authors declare no conflict of interest.

References

1. Feng, L.; Yan, H. Nonlinear Adaptive Robust Control of the Electro-Hydraulic Servo System. *Appl. Sci.* **2020**, *10*, 4494. [CrossRef]
2. Nguyen, M.H.; Dao, H.V.; Ahn, K.K. Adaptive Robust Position Control of Electro-Hydraulic Servo Systems with Large Uncertainties and Disturbances. *Appl. Sci.* **2022**, *12*, 794. [CrossRef]
3. Lin, S.; An, G.; Huang, J.; Guo, Y. Robust Backstepping Control with Active Damping Strategy for Separating-Metering Electro-Hydraulic System. *Appl. Sci.* **2020**, *10*, 277. [CrossRef]
4. Guo, K.; Wei, J.; Tian, Q. Nonlinear adaptive position tracking of an electro-hydraulic actuator. *Proc. Inst. Mech. Eng. Part C J. Mech. Eng. Sci.* **2015**, *229*, 3252–3265. [CrossRef]
5. Feng, H.; Qiao, W.; Yin, C.; Yu, H.; Cao, D. Identification and compensation of non-linear friction for a electro-hydraulic system. *Mech. Mach. Theory* **2019**, *141*, 1–13. [CrossRef]
6. Guo, K.; Li, M.; Shi, W.; Pan, Y. Adaptive Tracking Control of Hydraulic Systems with Improved Parameter Convergence. *IEEE Trans. Ind. Electron.* **2022**, *69*, 7140–7150. [CrossRef]
7. Ding, R.; Cheng, M.; Jiang, L.; Hu, G. Active Fault-Tolerant Control for Electro-Hydraulic Systems with an Independent Metering Valve Against Valve Faults. *IEEE Trans. Ind. Electron.* **2021**, *68*, 7221–7232. [CrossRef]
8. Li, Z.; Wang, C.; Quan, L.; Hao, Y.; Ge, L.; Xia, L. Study on energy efficiency characteristics of the heavy-duty manipulator driven by electro-hydraulic hybrid active-passive system. *Automat. Constr.* **2021**, *125*, 103646. [CrossRef]
9. Jing, C.; Xu, H.; Jiang, J. Practical torque tracking control of electro-hydraulic load simulator using singular perturbation theory. *ISA Trans.* **2020**, *102*, 304–313. [CrossRef]
10. Du, H.; Shi, J.; Chen, J.; Zhang, Z.; Feng, X. High-gain observer-based integral sliding mode tracking control for heavy vehicle electro-hydraulic servo steering systems. *Mechatronics* **2021**, *74*, 102484. [CrossRef]
11. Wang, C.; Jiao, Z.; Wu, S.; Shang, Y. Nonlinear adaptive torque control of electro-hydraulic load system with external active motion disturbance. *Mechatronics* **2014**, *24*, 32–40. [CrossRef]
12. Lin, C.; Shen, F.; Wu, K.; Lee, H.; Hwang, S. Injection Molding Process Control of Servo–Hydraulic System. *Appl. Sci.* **2020**, *10*, 71. [CrossRef]
13. Hua, Z.; Rong, X.; Li, Y.; Chai, H.; Li, B.; Zhang, S. Analysis and Verification on Energy Consumption of the Quadruped Robot with Passive Compliant Hydraulic Servo Actuator. *Appl. Sci.* **2020**, *10*, 340. [CrossRef]
14. Chen, X.; Zheng, F.; Gan, W.; Xing, S. Exploration and Research on Key Technologies for Improving the Response Speed of Servo-Hydraulic Cylinders. *Appl. Sci.* **2022**, *12*, 4162. [CrossRef]
15. Sidhom, L.; Chihi, I.; Smaoui, M. Automation of a Hybrid Control for Electrohydraulic Servo-Actuators with Residual Dynamics. *Appl. Sci.* **2022**, *12*, 2856. [CrossRef]
16. Wei, J.; Guo, K.; Fang, J.; Tian, Q. Nonlinear supply pressure control for a variable displacement axial piston pump. *Proc. Inst. Mech. Eng. Part I J. Syst. Control Eng.* **2015**, *229*, 614–624. [CrossRef]
17. Ge, L.; Dong, Z.; Huang, W.; Quan, L.; Yang, J.; Li, W. Research on the Performance of Hydraulic Excavator with Pump and Valve Combined Separate Meter in and Meter out Circuits. In Proceedings of the 2015 international conference on fluid power and mechatronics (FPM), Harbin, China, 5–7 August 2015.
18. Tunay, I.; Rodin, E.Y.; Beck, A.A. Modeling and robust control design for aircraft brake hydraulics. *IEEE Trans. Contr. Syst. Trans.* **2001**, *9*, 319–329. [CrossRef]
19. Hongliu, D. Pressure Control with Power Limitation for Hydraulic Variable Displacement Piston Pumps Hongliu Du. In Proceedings of the 2002 American Control, Anchorage, AK, USA, 8–10 May 2002; pp. 940–945.
20. Parker, N.R.; Salcudean, S.E.; Lawrence, P.D. Application of Force Feedback to Heavy Duty Hydraulic Machines. In Proceedings of the [1993] Proceedings IEEE International Conference on Robotics and Automation, Atlanta, GA, USA, 2–6 May 1993.
21. Zhu, C.; Zhang, H.; Wang, W.; Li, K.; Zhou, Z.; He, H. Compound Control on Constant Synchronous Output of Double Pump-Double Valve-Controlled Motor System. *Processes* **2022**, *10*, 528. [CrossRef]

22. Yu, B.; Zhu, Q.; Yao, J.; Zhang, J.; Huang, Z.; Jin, Z.; Wang, X. Design, Mathematical Modeling and Force Control for Electro-Hydraulic Servo System with Pump-Valve Compound Drive. *IEEE Access* **2020**, *8*, 171988–172005. [CrossRef]
23. An, G.; Peng, Z.; Fu, Y. The Application of Predictive Functional Control to New Motor Pump-Valve Compound Control System. In Proceedings of the 2009 9th International Conference on Electronic Measurement & Instruments, Beijing, China, 16–19 August 2009.
24. Ding, H.; Zhao, J.; Cao, C.; Zhao, L. Valve–pump parallel variable mode control for hydraulic speed regulation of high-power systems. *Adv. Mech. Eng.* **2017**, *9*, 2071941856. [CrossRef]
25. Ding, H.; Zhao, J. Performance analysis of variable speed hydraulic systems with large power in valve-pump parallel variable structure control. *J. Vibroeng.* **2014**, *16*, 1042–1062.
26. Komsta, J.; van Oijen, N.; Antoszkiewicz, P. Integral sliding mode compensator for load pressure control of die-cushion cylinder drive. *Control Eng. Pract.* **2013**, *21*, 708–718. [CrossRef]
27. Guo, K.; Wei, J.; Fang, J.; Feng, R.; Wang, X. Position tracking control of electro-hydraulic single-rod actuator based on an extended disturbance observer. *Mechatronics* **2015**, *27*, 47–56. [CrossRef]
28. Tian, Q.; Wei, J.; Fang, J.; Guo, K. Adaptive fuzzy integral sliding mode velocity control for the cutting system of a trench cutter. *Front. Inf. Technol. Electron. Eng.* **2016**, *17*, 55–66. [CrossRef]
29. Komsta, J.; Adamy, J.; Antoszkiewicz, P. Input-Output Linearization and Integral Sliding Mode Disturbance Compensation for Electro-hydraulic Drives. In Proceedings of the 2010 11th International Workshop on Variable Structure Systems (VSS), Mexico City, Mexico, 26–28 June 2010.
30. Liu, S.; Yao, B. Automated onboard modeling of cartridge valve flow mapping. *IEEE/ASME Trans. Mechatron.* **2006**, *11*, 381–388.
31. Kemmetmüller, W.; Fuchshumer, F.; Kugi, A. Nonlinear pressure control of self-supplied variable displacement axial piston pumps. *Control Eng. Pract.* **2010**, *18*, 84–93. [CrossRef]
32. Yun, J.N.; Su, J. Design of a Disturbance Observer for a Two-Link Manipulator with Flexible Joints. *IEEE Trans. Contr. Syst. Trans.* **2014**, *22*, 809–815. [CrossRef]
33. Merritt, H.E. *Hydraulic Control Systems*; Wiley: Hoboken, NJ, USA, 1967.
34. Guo, K.; Wei, J. Adaptive Robust Control of Variable Displacement Pumps. In Proceedings of the 2013 American Control Conference, Washington, DC, USA, 17–19 June 2013.
35. Sun, J.; Kolmanovsky, I.V. Load governor for fuel cell oxygen starvation protection: A robust nonlinear reference governor approach. *IEEE Trans. Contr. Syst. Trans.* **2005**, *13*, 911–920.